Supplementary

Eight specific signs

- Enlarged radial crest with sclerotic margins and rough surfaces (*Figure 2*)
- Ossification of the ulnar-radial interosseous membrane (A)
- Loosening of attachment of pronator teres (B)
- Ossification of the tendon of the musculus soleus (C)
- Ossification of the interosseous membrane of the tibiofibular ossicle (D)
- Ossification of the obturator foramen membrane (E)
- Ossification of the sacrotuberous ligament (F)
- Ossification of the sacrospinous ligament (G)

The particular subjective assessment scoring criteria are as follows:

- FI-RADS 1: Very low probability, extremely unlikely to exist;
- FI-RADS 2: Low probability, unlikely to exist;
- FI-RADS 3: Moderate possibility, suspicious presence;
- FI-RADS 4: High probability, may be present;
- FI-RADS 5: Very high, highly likely to exist.

A FI-RADS score of 4 or 5 should be considered skeletal fluorosis.

https://dx.doi.org/10.21037/qims-2025-1-2773

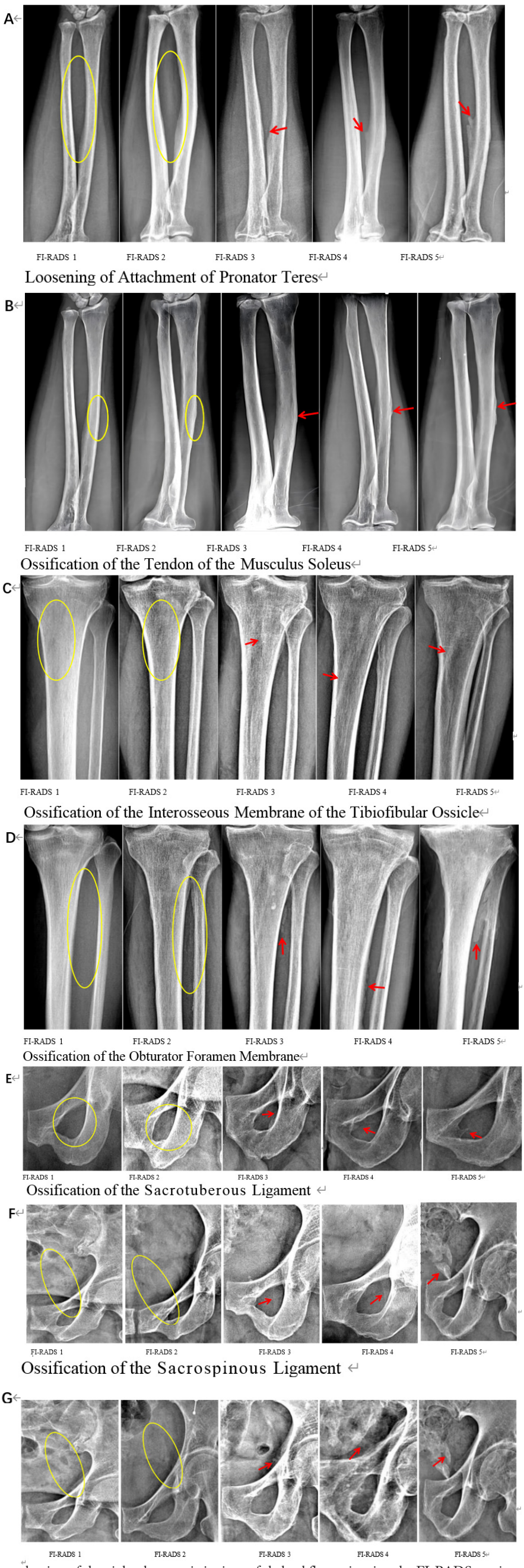

Figure S1 Subjective evaluation of the eight characteristic signs of skeletal fluorosis using the FI-RADS scoring system. FI-RADS, Fluorosis Imaging Reporting and Data System.

https://dx.doi.org/10.21037/qims-2025-1-2773

Table S1 Spline-based analysis of the nonlinear association between age and typical radiographic features of skeletal fluorosis stratified by FI-RADS scores (>3)

Radiological features	Total (n)	R^2	Model χ^2	Nonlinear P value	Optimal risk threshold (years)	Effect size (95% CI)
Radial crest	453	0.03	9.08	0.01	50	0.61 (0.21-1.00)
Ulnar-radial interosseous membrane	453	0.04	7.83	0.02	77	0.49 (0.20-0.78)
Attachment of pronator teres	453	0.15	54.38	<0.0001	48	0.81 (0.29-1.33)
Tendon of the musculus soleus	453	0.04	12.23	0.01	48	0.63 (0.12-1.15)
Interosseous membrane of the tibiofibular ossicle	453	0.04	8.38	0.01	76	0.46 (0.19-0.73)
Sacrotuberous ligament	453	0.14	4.83	0.58	NA	NA
Sacrospinous ligament	453	0.06	4.42	0.08	NA	NA
Obturator foramen membrane	453	0.04	7.01	0.02	79	0.67 (0.33-1.01)

Effect size: at the inflection point of a non-linear age effect, the log odds ratio (log OR) associated with a one-year increase in age. NA: non-linear models are not applicable. R^2: R-squared. CI, confidence interval; FI-RADS, Fluorosis Imaging Reporting and Data System.

Table S2 Spline-based analysis of the nonlinear association between total bile acids and typical radiographic features of skeletal fluorosis stratified by FI-RADS scores (>3)

Radiological features	Total (n)	R^2	Model χ^2	Nonlinear P-value	Optimal risk threshold (μmol/L)	Effect size (95%CI)
Radial crest	428	0.18	5.90	0.17	NA	NA
Ulnar-radial interosseous membrane	428	0.07	13.59	0.001	3.00	0.38 (0.18-0.58)
Attachment of pronator teres	428	0.03	9.76	0.03	2.30	0.20 (0.01-0.39)
Tendon of the musculus soleus	428	0.03	7.92	0.03	2.30	0.29 (0.09-0.498)
Interosseous membrane of the tibiofibular ossicle	428	0.06	12.07	0.01	1.80	0.32 (0.12-0.52)
Sacrotuberous ligament	428	0.14	3.35	0.45	NA	NA
Sacrospinous ligament	428	0.01	0.41	0.76	NA	NA
Obturator foramen membrane	428	0.04	6.66	0.05	NA	NA

Note--Effect size: At the inflection point of a non-linear age effect, the log odds ratio (logOR) associated with a 1mol/L increase in total bile acids. NA: Non-linear models are not applicable. R^2: R-squared. CI, confidence interval.

https://dx.doi.org/10.21037/qims-2025-1-2773

Appendix 1 Detailed FI-RADS scoring criteria for typical X-ray signs of skeletal fluorosis

S1. Radial crest

- Score 1: No enlargement of the radial crest, with clear and sharp borders.
- Score 2: No enlargement of the radial crest, with unclear boundaries (slightly blurred or rough).
- Score 3: The radial crest is enlarged, with clear or slightly blurred boundaries.
- Score 4: The radial crest is significantly enlarged, accompanied by marginal sclerosis and/or surface blurring (bone structure is unclear).
- Score 5: Significant enlargement of the radial crest, accompanied by marginal sclerosis and surface blurring (unclear bone structure).

S2. Ulnar-radial interosseous membrane

- Score 1: No ossification is identified along the ulnar-radial interosseous membrane.
- Score 2: Isolated punctate or extremely short linear high-density shadows appear in the region of the ulna-radius interosseous membrane, with low density (faint) and blurred boundaries.
- Score 3: Continuous fine linear ossification shadows appear in the area between the radius and ulna, with moderate density and relatively clear boundaries.
- Score 4: "Sprouting bud-like" bone spurs appear in the interosseous membrane region of the radius and ulna, with thickened ossification shadows and clear boundaries.
- Score 5: "Rose thorn-like" ossification shadows appear in the interosseous membrane region of the radius and ulna, which may be accompanied by irregular edges or fusion with adjacent bone tissue.

S3. Attachment of pronator teres

- Score 1: The anterior lateral cortex of the middle and upper segments of the radius is smooth and dense, with a clear and continuous trabecular structure and no signs of resorption.
- Score 2: Small lucent areas are seen in the subcortical region, with a density slightly lower than that of the surrounding bone, blurred boundaries, and a slightly rough cortical surface.
- Score 3: Localized subcortical lucent lesions with clear/partially blurred borders, a mildly rough cortex but no stratification, and an unclear transition between areas of reduced density and adjacent bone.
- Score 4: "Flame-shaped" translucent area, cortical layering, sieve-like changes along the tendons.
- Score 5: Localized disruption of the cortical bone, separation of the cortex from the cancellous bone, and irregular or "worm-eaten" changes in the endosteal surface.

S4. Tendon of the musculus soleus

- Score 1: No abnormal high-density shadows in the region of the posterior tibial tendon, soft tissue layers are clear, and the tibial cortex is smooth with no osteophytes.
- Score 2: Localized scattered punctate/patchy calcification, but characteristics are inconsistent (e.g., location deviates from tendon course, more consistent with vascular calcification/cartilage calcification).
- Score 3: A blurred linear high-density shadow is observed along the tendon course, with varying density, unclear and irregular borders, and no clear connection to the bone.
- Score 4: A linear area of high density consistent with the course of the soleus muscle tendon, with a uniform increase in density.
- Score 5: A dense linear shadow consistent with the course of the soleus muscle tendon, attached at one end to the posterior margin of the tibia, with no bone marrow cavity penetrating through.

https://dx.doi.org/10.21037/qims-2025-1-2773

S5. Interosseous membrane of the tibiofibular ossicle

- Score 1: No abnormal high-density shadows in the tibia and fibula space; smooth bone cortex without hyperplasia.
- Score 2: Scattered punctate/patchy calcification, located away from the interosseous membrane, more consistent with vascular calcification/dystrophic calcification.
- Score 3: Discontinuous linear high-density shadows are observed along the interosseous membrane, with varying density and uneven distribution, not connecting to the cortical bone of the tibia and fibula.
- Score 4: A slightly higher density shadow running along the tibiofibular interval, appearing as parallel shadows resembling railroad tracks.
- Score 5: Continuous strip-like high-density shadows running along the tibia and fibula, ossification bands fused with the cortical bone, and edges may appear wavy.

S6. Obturator foramen membrane

- Score 1: No abnormal high-density shadows in the closed area; the bone cortex at the attachment site of the closed membrane is continuous and smooth.
- Score 2: Scattered punctate or patchy calcifications in the obturator membrane region, located away from the anatomical course of the obturator membrane (not distributed along the obturator margin), with variable density, more consistent with vascular calcification or nutritional deficiency calcification.
- Score 3: Discontinuous linear faint high-density shadows are observed along the closed membrane, with uneven density, but cannot be clearly distinguished from artifacts/nonspecific calcification, and do not meet the criteria for definite ossification.
- Score 4: Continuous strip-like high-density shadows running along the closed membrane, appearing as parallel shadows resembling "railroad tracks" with transparent gaps between the shadows and the bone cortex.
- Score 5: The ossification zone is fused with the periosteum around the obturator foramen, with dense and uniform density and wavy/spiny protrusions at the edges.

S7. Sacrospinous ligament

- Score 1: No abnormal high-density shadows between the lateral margin of the sacrum and the ischial spine.
- Score 2: Scattered punctate/patchy calcifications in the course of the sacral spinous ligament, deviating from the main trunk of the sacral spinous ligament.
- Score 3: Discontinuous, faint linear shadows are seen along the course of the ligament, but artifacts or calcification cannot be ruled out, and no continuous bands are formed.
- Score 4: Continuous, high-density linear shadows connecting the sacrum and the ischial spines, with lucent gaps between the shadows and the bone cortex.
- Score 5: The ossification zone is fused with the sacrum/ischial spine cortex to form a single unit, with a density similar to that of cortical bone and spiny projections at the edges.

S8. Sacrotuberous ligament

- Score 1: No abnormal high-density shadows between the sacrum and the ischial tuberosity.
- Score 2: Scattered punctate/patchy calcifications in the sacral spinous ligament region, deviating from the main trunk of the sacral tubercle ligament.
- Score 3: Discontinuous, faint linear shadows are seen along the course of the ligament, but artefacts or calcification cannot be ruled out, and no continuous bands are formed.
- Score 4: Continuous, high-density shadows connecting the sacrum and ischial tuberosity, with a clear gap between the shadows and the bone cortex.
- Score 5: The ossification zone is fused with the cortical bone of the sacrum/ischial tuberosity, with the same density as cortical bone, and the edges form spinous processes.

https://dx.doi.org/10.21037/qims-2025-1-2773